UNCLASSIFIED

WATERTOWN ARSENAL LABORATORY

MEMORANDUM REPORT

NO. WAL 710/676

Metallurgical Examination of Sections from Two 4 Inch Thick Cast Armor Plates Manufactured by Continental Foundry and Machine Company

BY

N. A. MATTHEWS
Major, Ordnance Dept.

DATE 14 July 1944

WATERTOWN ARSENAL
WATERTOWN, MASS.

UNCLASSIFIED

WATERTOWN ARSENAL LABORATORY

MEMORANDUM REPORT NO. WAL 710/676

Final Report on Problem B-4.39

14 July 1944

Metallurgical Examination of Sections from Two 4 Inch Thick Cast Armor Plates Manufactured by Continental Foundry and Machine Company

ABSTRACT

Sections from two plates, cast from the same heat and heat treated identically behaved altogether differently under ballistic test, one plate failing badly whereas the second was satisfactory. Failure of the poor plate was attributed to poor shock properties as indicated by crystalline fracture and poor impact values. Surface network crack system on both plates, but more pronounced on plate which failed, was severely oxidized indicating that defect formed upon solidification because of a poor mold condition. The poor shock properties of the failing plate are attributed to temper embrittlement.

1. At the request of the Ordnance Research Center, Aberdeen (reference Memorandum Report dated 28 April 1944 covering the acceptance test of two 4 inch plates under Specification AXS-1013), samples from two plates submitted by Continental Foundry and Machine Company were forwarded to the laboratory for metallurgical examination. The two plates were cast from the same heat of steel (Number 2123) at the Wheeling, West Virginia plant and were presumably heat treated simultaneously and nominally identically. However, under ballistic test one plate (2123-4) was completely satisfactory whereas the second plate (2123-1) failed badly both on the shock test because of a complete penetration with a large back spall and excessive cracking and also on resistance to penetration.

2. Metallurgical examination consisted of the following tests:

a. Fibre fracture tests.

b. Macroetch tests.

c. Brinell hardness across sections.

d. V-notch Charpy impact tests.

e. Microscopic examination.

3. The detailed results of the examinations appear below:

a. Fibre fracture test. The samples as-received were notched deeply and broken by the impact blow of a forge hammer. Plate 2123-1 showed a mottled, completely crystalline fracture. A surface network effect visible on the unmachined plate surface was caused by oxidized cracks extending in perpendicular to the surface to a distance of from 1/8 to 3/16 inches. Plate 2123-4 (which passed the ballistic test satisfactorily) developed an essentially fibrous fracture containing not over 5% of scattered crystallinity in the central third of the section which is probably attributable to segregation effects. No continuous surface network was visible on the face of the plate, but the fracture showed evidence that the same defect was present to a smaller degree. The extreme difference in shock properties of the two plates, as exemplified by the greatly different fracture appearances, is directly associated with the observed variability in ballistic shock test behavior.

b. Macroetch tests. Macroetch tests were made of the full section of each plate. The photographic results appear as Figure 1. It will be observed that the two plates are very similar in macro appearance and both are extremely sound. The surface defect is plainly visible on one face of each plate. The etched original plate face of these sections showed a continuous network of the cracks illustrated. Such cracks would form stress concentrations if on the back face of the plate during testing, but it is not considered that this condition was the primary cause of the observed differences in ballistic behavior.

c. Brinell hardness tests. Brinell hardness surveys were made across the thickness of each plate. Twelve impressions were made at equally spaced intervals on a carefully ground surface. The results obtained are as follows:

Plate Number	Range BHN	Average BHN
2123-1	229-241	235
2123-4	229-241	234

Hardnesses were sufficiently uniform across the sections to indicate complete quench hardening. The plates are very comparable with respect to hardness.

d. V-notch Charpy impact tests. Four V-notch Charpy impact test specimens were cut from each plate section in such a manner that the axis of the specimens corresponded to the location midway between the surface and center of the sections. Two specimens each from each plate section were tested at 68°F (20°C) and -40°F (-40°C). The results are shown below:

V-notch Charpy Impact Results

Plate Number	Room Temperature Tests		Tests at -40°F	
	Ft. Lbs.	Fracture*	Ft. Lbs.	Fracture*
2123-1	46.5	Fc	16.5	Cb
	45.8	Fc	14.9	Cb
2123-4	83.0	F	54.2	Fc
	77.5	F	51.3	Fc

*F - fibrous   Fc - fibrous with scattered crystallinity
Cb - bright crystalline

The great differences in shock properties of the two plates, confirming the fracture test results, are indicated by the relative impact values at the -40°F testing temperature. The impact values of the satisfactory plate material (2123-4) are perfectly satisfactory for this hardness range, although the decrease in impact energy with the lowering of the test temperature is somewhat greater than would be expected from tempered martensite devoid of temper embrittlement.

e. Microscopic examination. A detailed metallographic study was made of the characteristics of the surface crack system which was common to both plates but which was more extensive in the case of plate 2123-1. In addition, the microstructures of the two plates were compared. Figure 2A shows a photomicrograph at low magnification of the nature of the surface cracks or checks which were common to both plates. It will be observed that the cracks are filled with iron oxide and that the metal around the crack systems is severely decarburized. Figure 2 also shows the microstructures of the two plates at the center of the sections. Both structures appear satisfactory and very similar. Examination of the microstructure alone would lead to the expectancy that the shock properties of the two plates would be satisfactory and comparable.

Figure 3 shows a panorama of a typical crack system at the surface of plate 2123-1. It will be observed that the crack is filled with iron oxide, and that, surrounding the crack, there is a considerable zone which contains iron oxide particles randomly distributed. Figure 4C shows a detail of the globular iron oxides surrounding the cracks, and Figure 4D shows the complete decarburization to ferrite of the metal adjacent to the cracks.

4. The analysis of the heat of steel from which these plates were poured is as follows:

Heat No.	C	Mn	Si	S	P	Cr	Ni	Mo	V
2123	.29	1.29	.35	.023	.033	1.21	1.48	.50	.09

Such an analysis has adequate hardenability to quench harden in a 4 inch section, and the microstructure indicates that complete quench hardening was obtained. The ballistic results on the satisfactory plate (2123-4) have proven that this steel, if properly heat treated, will produce satisfactory shock properties. The failure of the second plate (2123-1) could possibly be attributed to one of two causes: (1) stopping the quench before transformation had been completed and immediately tempering or (2) temper embrittlement caused by too slow a cool from the tempering temperature. The equivalence in hardness and the similarity in microstructure of the two plates lent greater credence to the latter factor as being responsible for the poor behavior. In order to demonstrate that temper embrittlement was involved, a small section from sample 2123-1 was retempered for one hour at 1200°F and water quenched. The fracture after this treatment was completely fibrous. Temper embrittlement is highly probable in a steel of this type (high in manganese and chromium and containing vanadium) when air cooled from the temper in a 4 inch section. It is probable that the fracture and impact properties of the satisfactory plate (2123-4) were partially impaired by the air cooling treatment from the tempering temperature.

The surface network effect of oxidized cracks found on both plates undoubtedly resulted from some unsatisfactory mold condition. It is certain that the cracks were present prior to homogenization of the casting, since such oxidation adjacent to crack systems can occur only at high temperatures (in this case 2000°F). The regularity of the network condition is puzzling and suggests that the cracks follow the original as-cast grain boundaries. This would suggest that the effect was caused by a poor mold condition.

5. The extreme differences in shock properties of these two plates (poured from the same heat of steel and heat treated nominally identically) indicate the fallacy of basing the ballistic acceptance of shield castings on the ballistic performance of test plates. The complete validity of the fibre fracture test is again confirmed. It is necessary that heavy armor castings be essentially fibrous to yield satisfactory ballistic properties and the only practicable way of guaranteeing satisfactory shock properties on such castings is by a strict application of the fibre fracture test.

N. A. Matthews

N. A. MATTHEWS
Major, Ordnance Dept.
Chief, Armor Section

MACROETCH TESTS

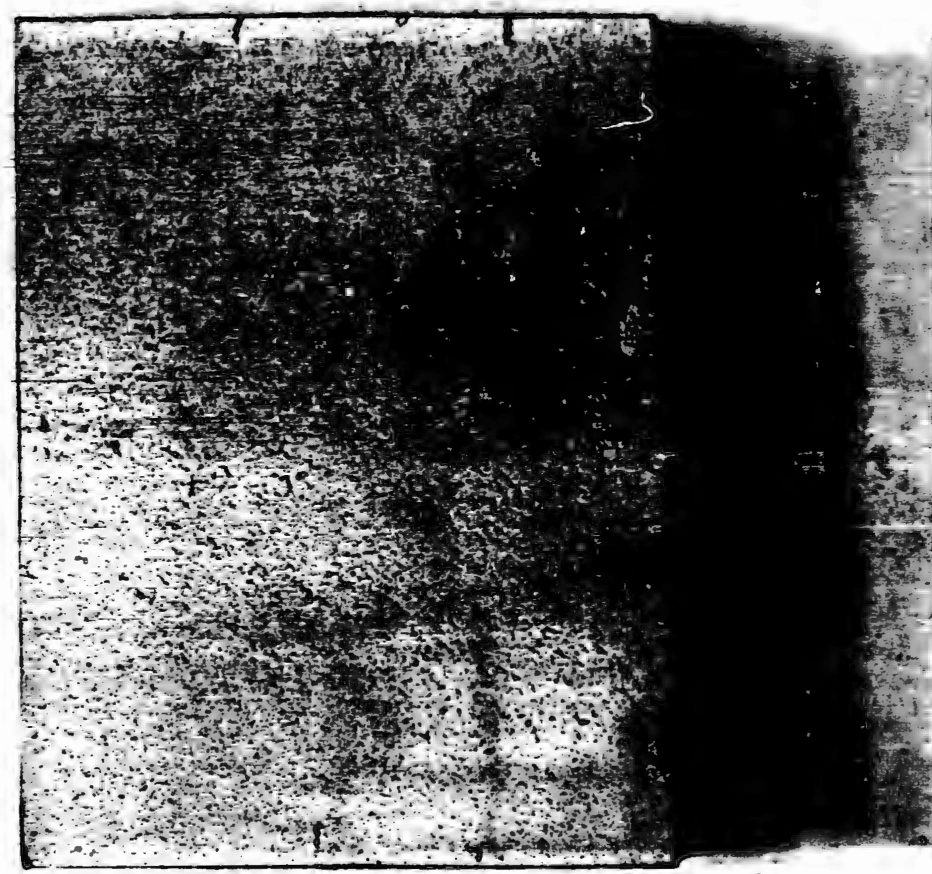

PLATE 1, HEAT 2123

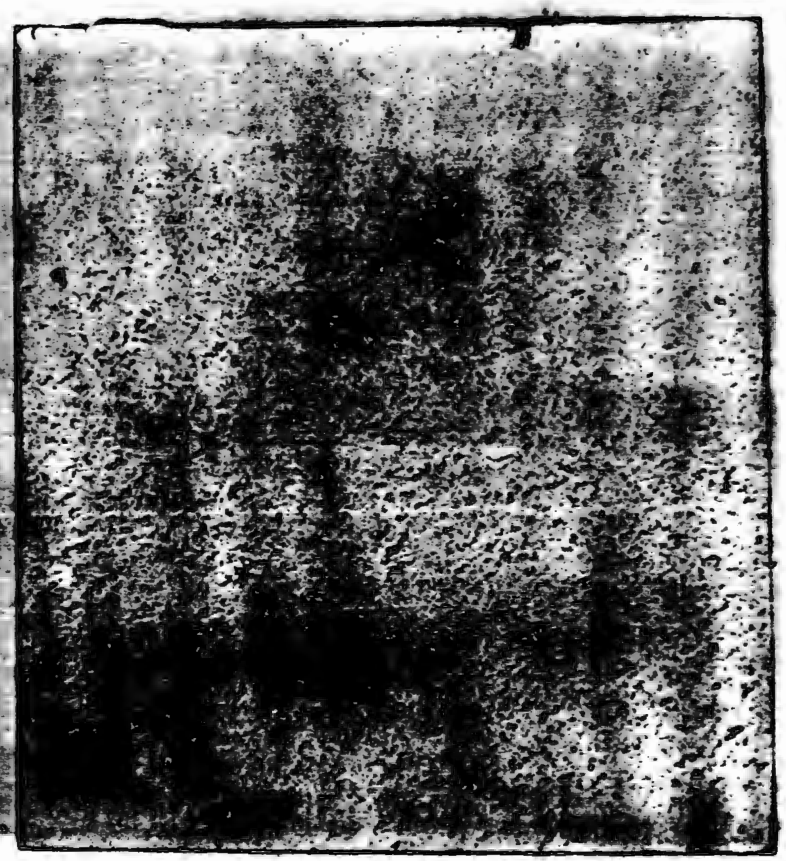

PLATE 4, HEAT 2123

ORDNANCE DEPT. U.S.A.

CONTINENTAL FOUNDRY & MACHINE COMPANY 4" CAST ARMOR
20 JUNE 1944 WTN.710-2315

Fig. 1

Microstructures and Characteristics of Surface Defect

Deep Nital Etch **-A-** **Mag., X5**

Surface cracks in cast armor. Extensive decarburization around cracks.

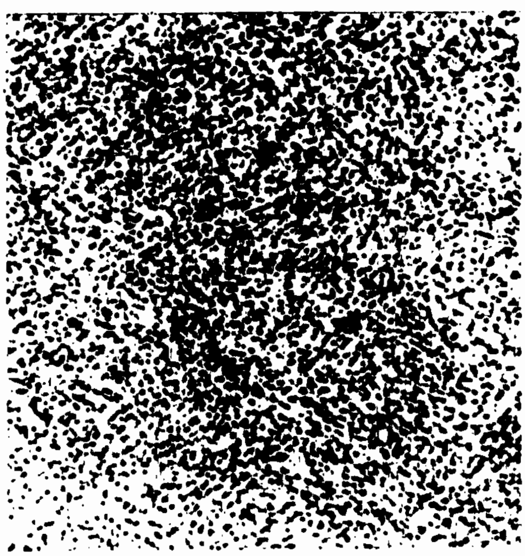

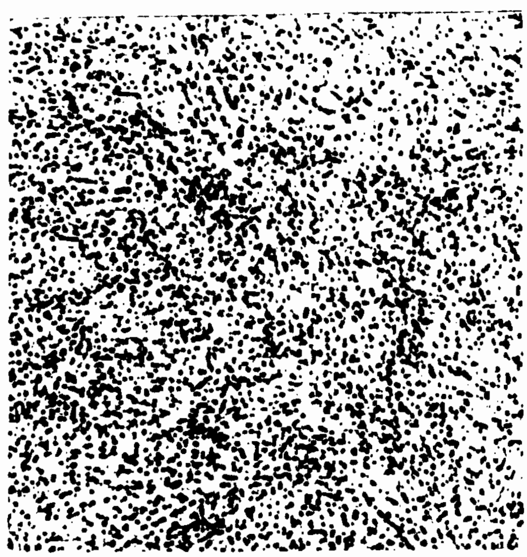

X1000 - Picral Etch

Plate 2123-1, Uniform tempered structure.

Plate 2123-4, Uniform tempered structure.

FIGURE

Panorama of Crack Systems

Unetched   1   Mag. X100

Surface cracks in cast armor. Oxides in cracks and heavy concentration of small globular oxides around cracks.

FIGURE 3.

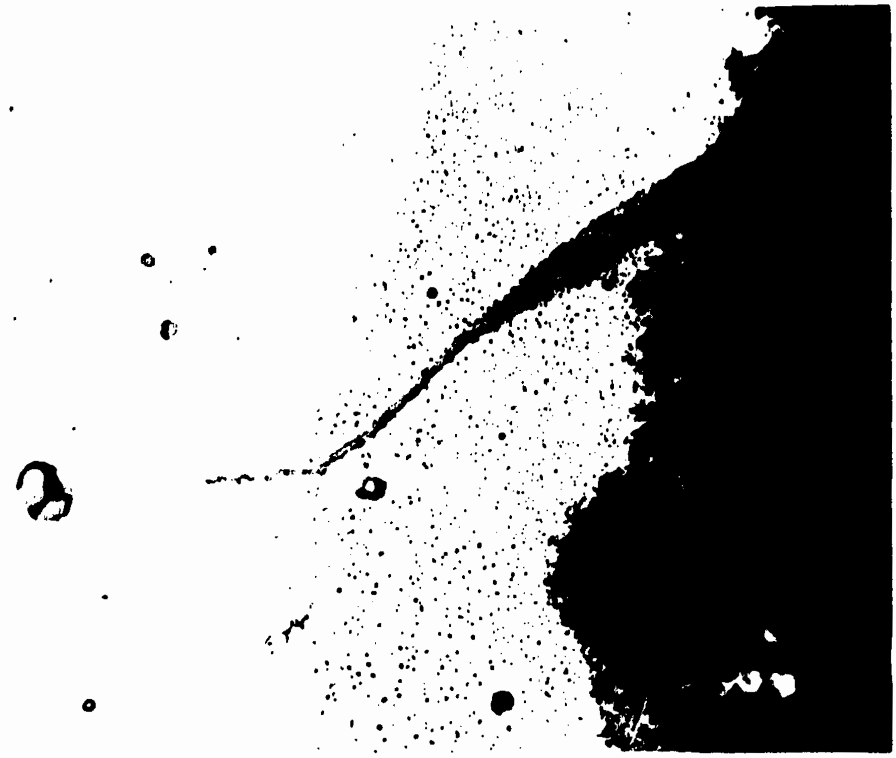

-C-

Unetched Mag. X250

High concentration of small globular oxides around crack.

-D-

Nital Etch. Same area as in previous photo. (B) Mag. X100

Areas rich in small globular oxides are darkened by etching.

Regions show complete decarburization to ferrite.

FIGURE 4.